

Influence of Cations on HCOOH and CO Formation during CO<sub>2</sub> Reduction on a PdMLPt(111) Electrode

*Original*

Influence of Cations on HCOOH and CO Formation during CO<sub>2</sub> Reduction on a PdMLPt(111) Electrode / Ye, Chunmiao; Dattila, Federico; Chen, Xiaoting; López, Núria; Koper, Marc T. M.. - In: JOURNAL OF THE AMERICAN CHEMICAL SOCIETY. - ISSN 0002-7863. - 145:36(2023), pp. 19601-19610. [10.1021/jacs.3c03786]

*Availability:*

This version is available at: 11583/2981890 since: 2023-09-11T07:43:16Z

*Publisher:*

American Chemical Society

*Published*

DOI:10.1021/jacs.3c03786

*Terms of use:*

This article is made available under terms and conditions as specified in the corresponding bibliographic description in the repository

*Publisher copyright*

(Article begins on next page)

# Influence of Cations on HCOOH and CO Formation during CO<sub>2</sub> Reduction on a Pd<sub>ML</sub>Pt(111) Electrode

Chunmiao Ye<sup>†, ||</sup>, Federico Dattila<sup>‡, §, ||</sup>, Xiaoting Chen<sup>†</sup>, Núria López<sup>‡</sup>, Marc T.M. Koper<sup>\*, †</sup>

<sup>†</sup> Leiden Institute of Chemistry, Leiden University, 2300 RA Leiden, The Netherlands

<sup>‡</sup> Institute of Chemical Research of Catalonia (ICIQ-CERCA), The Barcelona Institute of Science and Technology (BIST), 43007 Tarragona, Spain

<sup>§</sup> Present Address: Department of Applied Science and Technology (DISAT), Politecnico di Torino, Corso Duca degli Abruzzi 24, 10129 Turin, Italy.

<sup>||</sup> C.Y. and F.D. contributed equally to this work.

## Supporting Information

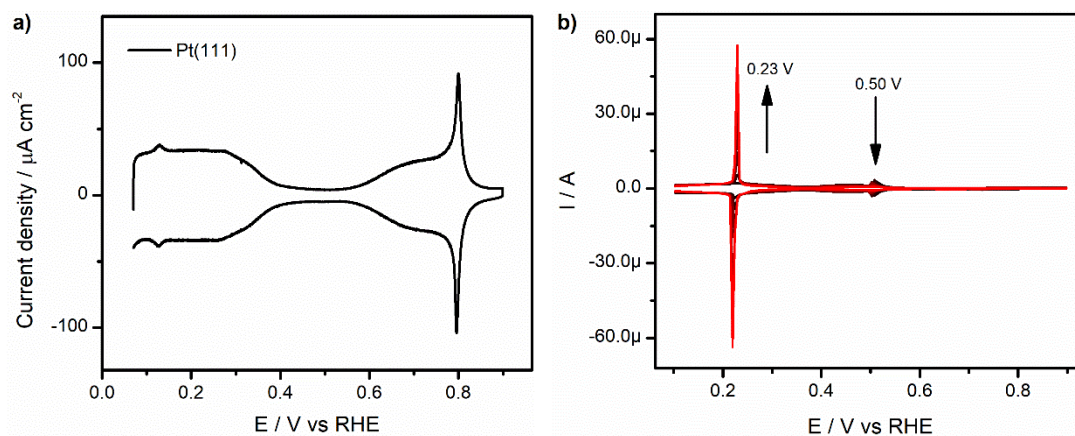


**Figure S1 a.** Cyclic voltammogram of Pt(111) in 0.1 M HClO<sub>4</sub>. Scan rate: 50 mV s<sup>-1</sup>. **b.** Cyclic voltammograms for Pt(111) in 0.1 M H<sub>2</sub>SO<sub>4</sub> + 0.1 mM PdSO<sub>4</sub>, recorded in successive stages during Pd deposition experiment. Scan rate: 50 mV s<sup>-1</sup>. Arrows indicate the evolution with time.

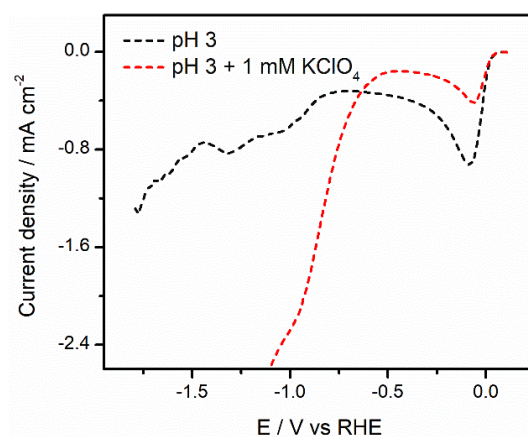


**Figure S2.** Linear Sweep Voltammetry of Pd<sub>ML</sub>Pt(111) in argon-purged pH 3 electrolytes in the absence (black) and presence of 1 mM KClO<sub>4</sub> (red). Scan rate: 10 mV/s.

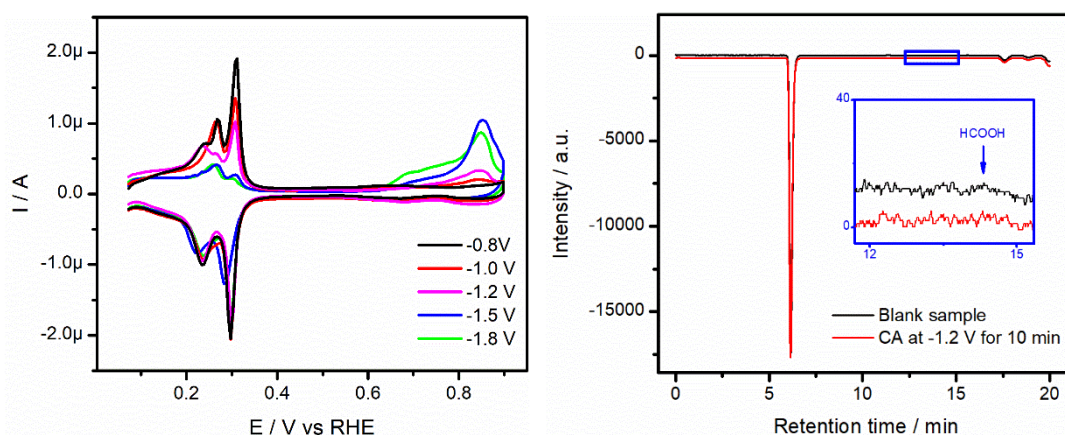


**Figure S3 a.** CO stripping voltammograms on Pd<sub>ML</sub>Pt(111) after CO<sub>2</sub> reduction at different vertex potentials in CO<sub>2</sub>-saturated pH 3 electrolyte without metal cations, measured at 10 mV s<sup>-1</sup>. **b.** HPLC data before and after chronoamperometry at -1.2 V<sub>RHE</sub> for 10 min in CO<sub>2</sub>-saturated pH 3 electrolyte without metal cations.

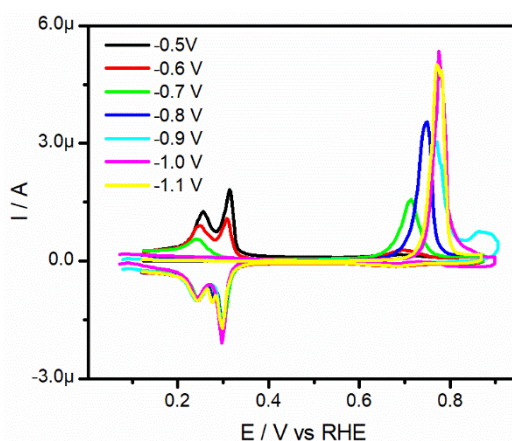


**Figure S4.** CO stripping voltammograms on Pd<sub>ML</sub>Pt(111) after CO<sub>2</sub> reduction at different vertex potentials in CO<sub>2</sub>-saturated pH 3 with 1 mM KClO<sub>4</sub> electrolyte, measured at 10 mV s<sup>-1</sup>.

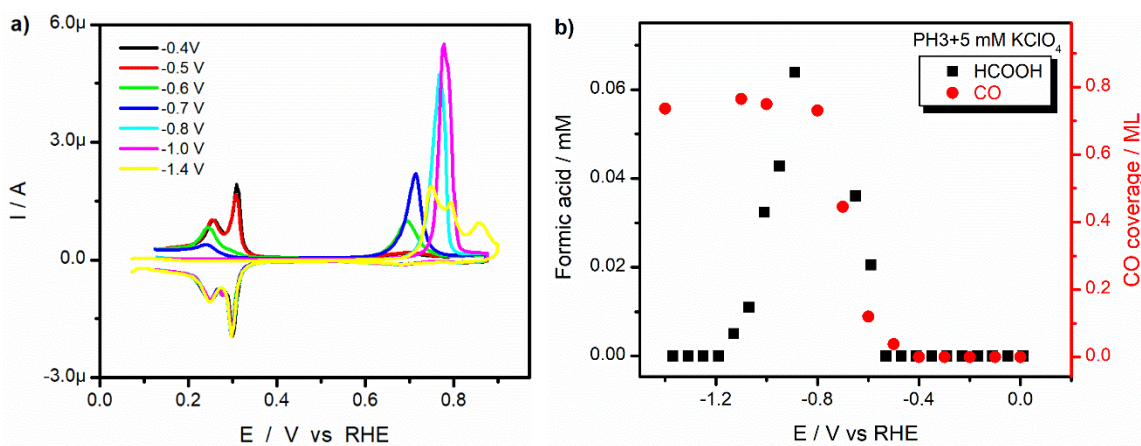


**Figure S5 a.** CO stripping voltammograms on Pd<sub>ML</sub>Pt(111) after CO<sub>2</sub> reduction at different vertex potentials in CO<sub>2</sub>-saturated pH 3 with 5 mM KClO<sub>4</sub> electrolyte, measured at 10 mV s<sup>-1</sup>. **b.** HCOOH formation and the calculated CO coverage as a function of potential.

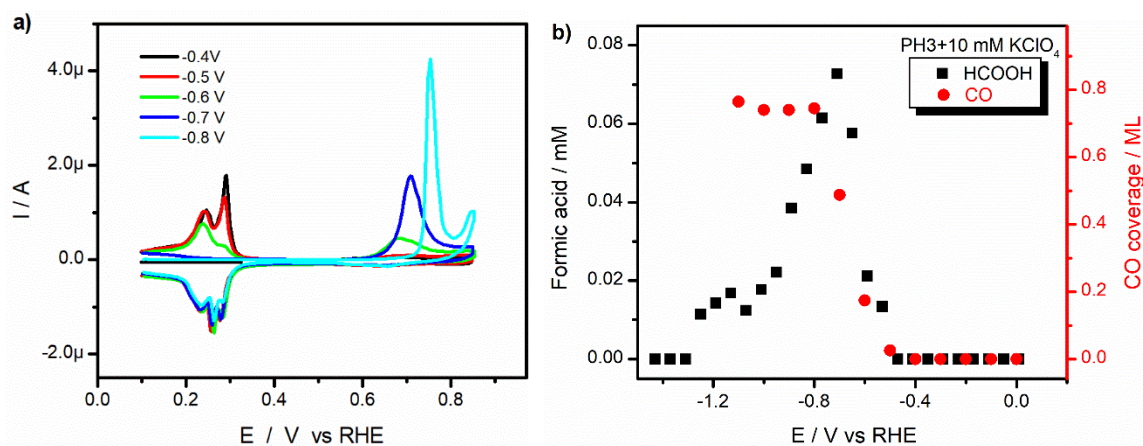


**Figure S6 a.** CO stripping voltammograms on Pd<sub>ML</sub>Pt(111) after CO<sub>2</sub> reduction at different vertex potentials in CO<sub>2</sub>-saturated pH 3 with 10 mM KClO<sub>4</sub> electrolyte, measured at 10 mV s<sup>-1</sup>. **b.** HCOOH formation and the calculated CO coverage as a function of potential.

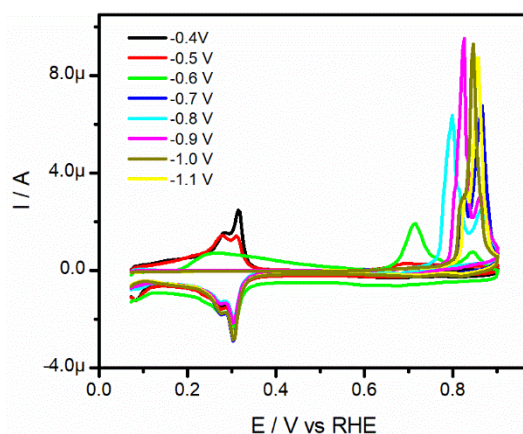


**Figure S7.** CO stripping voltammograms on Pd<sub>ML</sub>Pt(111) after CO<sub>2</sub> reduction at different vertex potentials in CO<sub>2</sub>-saturated pH 3 with 99 mM KClO<sub>4</sub> electrolyte, measured at 10 mV s<sup>-1</sup>.

Figures S3a, S4, S5a, S6a and S7 show oxidative stripping voltammograms of adsorbed CO obtained during CO<sub>2</sub>RR by increasing the vertex potential in steps of 0.1 V from -0.4 V<sub>RHE</sub>. With the positive going scan, decreasing peaks (peak at 0.31 V<sub>RHE</sub> decreasing first) in the potential region between +0.05 and +0.35 V<sub>RHE</sub> suggest adsorbed CO. CO<sub>ads</sub> oxidation peaks are observed in the potential region between +0.65 and +0.9 V<sub>RHE</sub>, the peaks varying under different conditions. These different CO oxidation peaks may result from different \*CO coverage or changes of local electrolyte after CO<sub>2</sub>RR. After oxidation of \*CO, the typical CV features in pH 3 electrolyte are again observed in the negative going scan. In some voltammograms, CV features of Pd<sub>ML</sub>Pt(111) slightly deviate from the standard, which might be due to minor loss of Pd atoms during CO<sub>2</sub>RR. Moreover, peaks in the potential region between +0.05 and +0.35 V<sub>RHE</sub> decreases with increasing of \*CO obtained from CO<sub>2</sub>RR, which leads to more CO oxidation current in potential region between +0.65 and +0.9 V<sub>RHE</sub> and corresponding higher CO coverage.

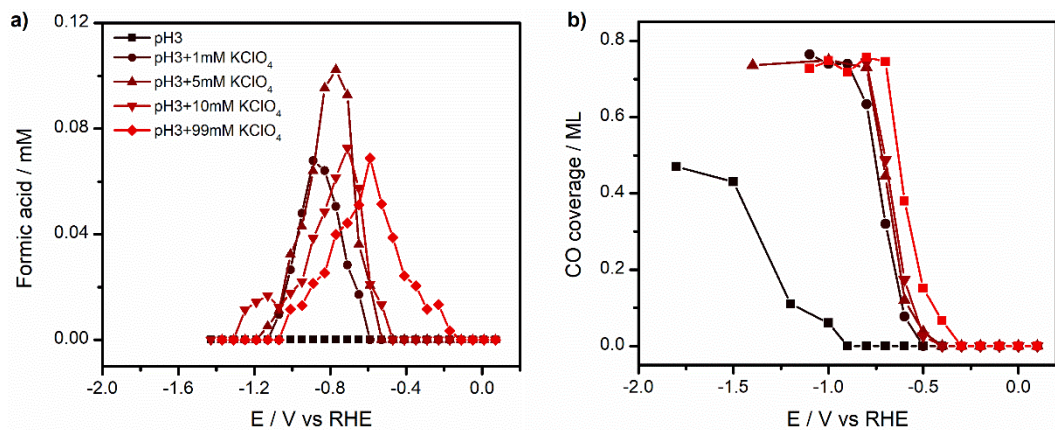


**Figure S8.** A summary of CO and formic acid generation during CO<sub>2</sub>RR in CO<sub>2</sub> saturated pH 3 electrolytes in the presence of 0, 1, 5, 10, 99 mM KClO<sub>4</sub>.

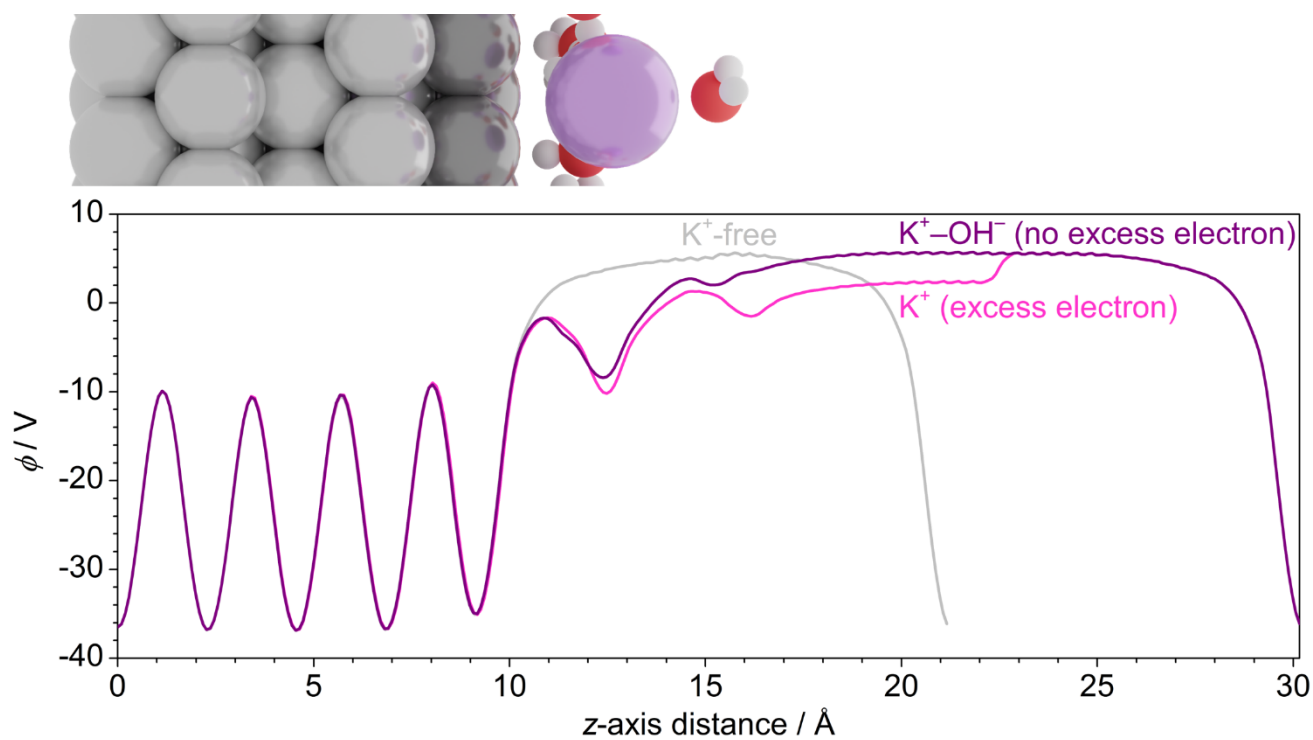


**Figure S9.** Electrostatic potential ( $\Phi$ ) profile across the simulation cell ( $z$ -direction, reported on top) for the cation-free (gray line) and near-cation ( $d_{K^+ \text{-surf}} = 4 \text{ \AA}$ ) systems with and without excess electron (magenta and purple line respectively).

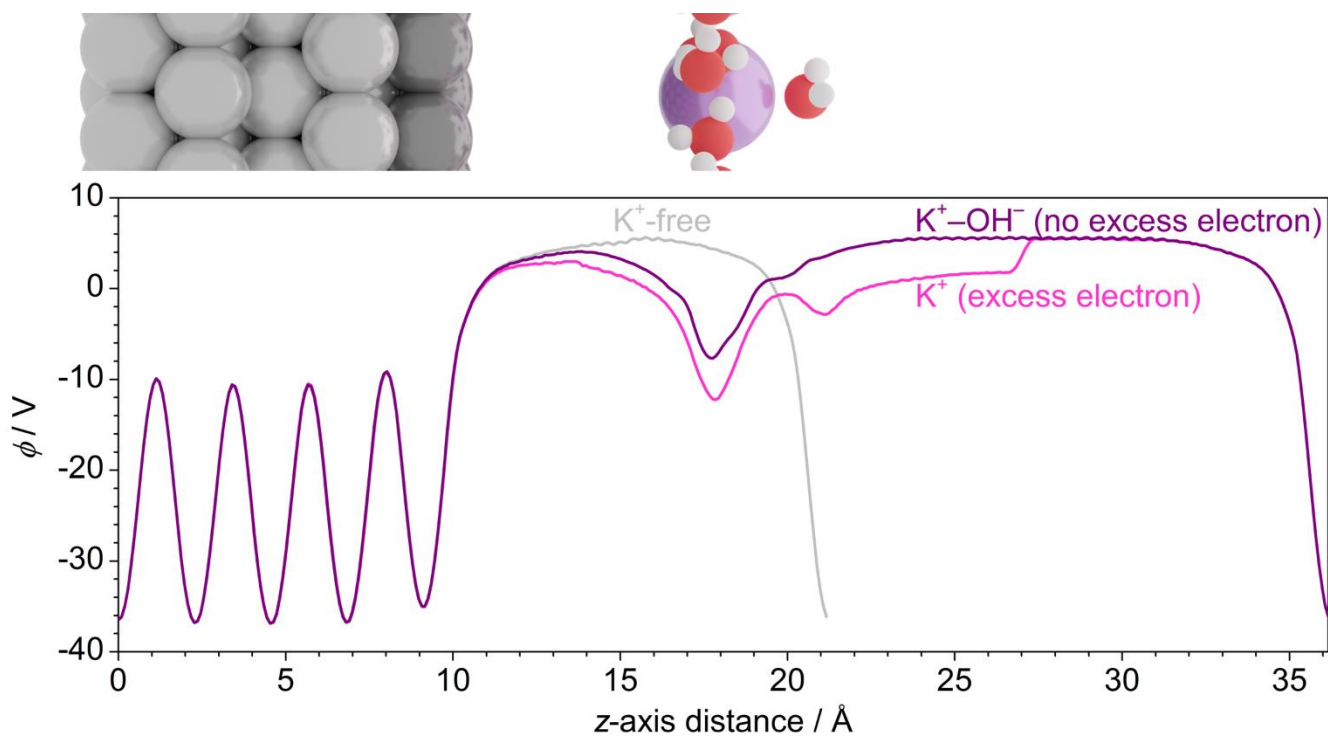


**Figure S10.** Electrostatic potential ( $\phi$ ) profile across the simulation cell ( $z$ -direction, reported on top) for the cation-free (gray line) and far-cation ( $d_{\text{K}^+ \text{-surf}} = 9 \text{ \AA}$ ) systems with and without excess electron (magenta and purple line respectively).

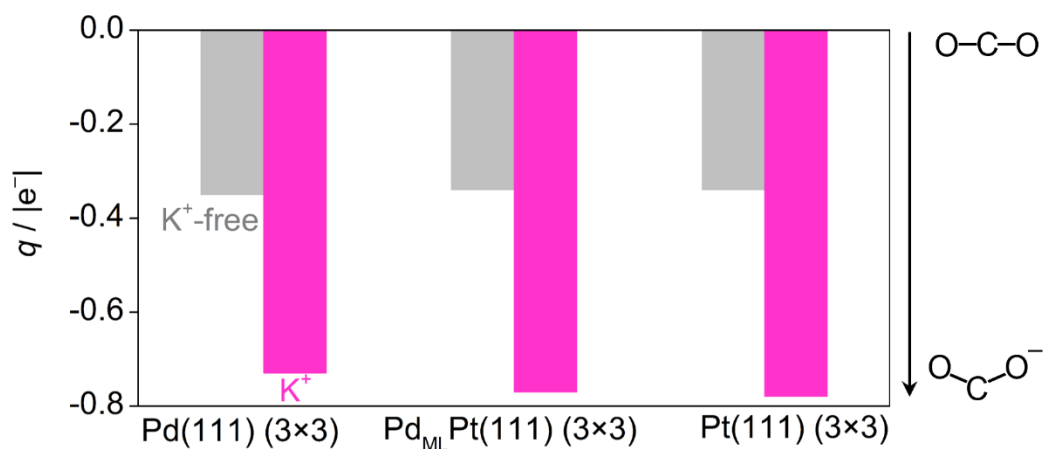


**Figure S11.** Bader charges for adsorbed  $\text{CO}_2^-$  on Pd(111) ( $3 \times 3$ ),  $\text{Pd}_{\text{ML}}\text{Pt}(111)$  ( $3 \times 3$ ), and Pt(111) ( $3 \times 3$ ). The gray column reports the baseline case for the adsorbate without  $\text{K}^+$ , while the near- $\text{K}^+$  system (with excess electron) is indicated in magenta. Solvated  $\text{K}^+$  was here simulated with three water molecules within its coordination shell.

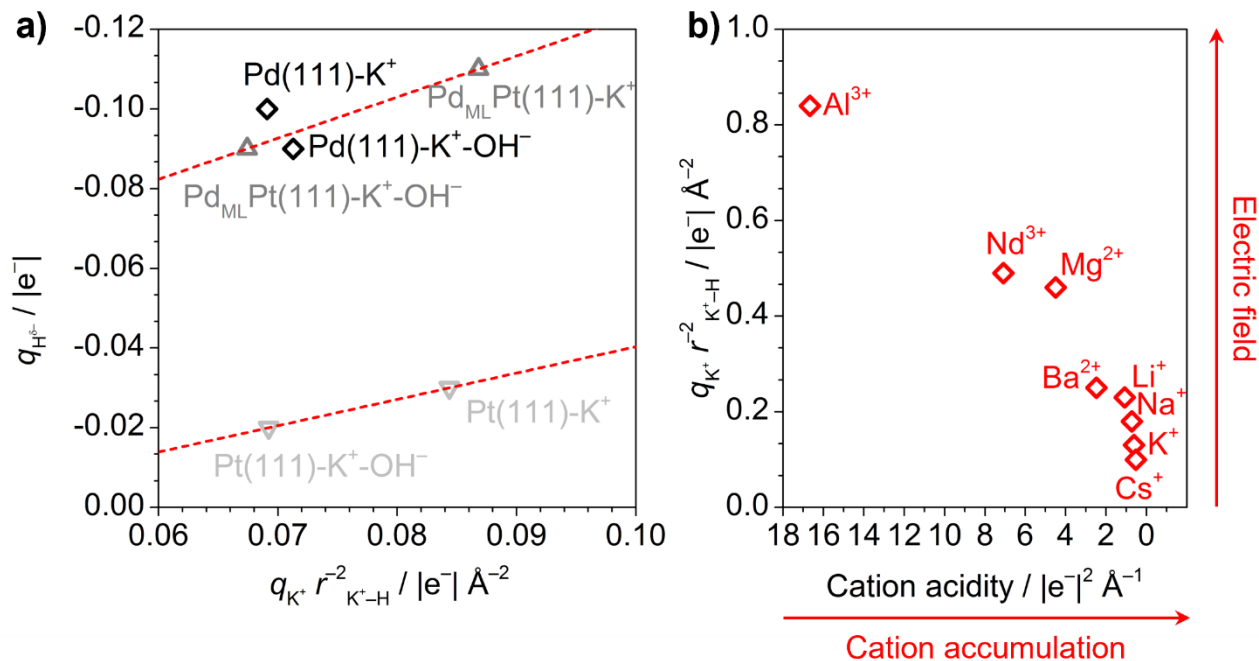


**Figure S12.** a. Correlation between H<sup>δ-</sup> Bader charges and cation-induced electric field, proportional to  $q^{K^+}/r_{K^+-H}^2$ . b. Cation-induced electric field vs cation acidity for alkali, bi-valent, and tri-valent cations. Cation acidity affects cation accumulation, while electric field favors the formation of hydrides on the surface. The distance between cation and hydrogen is here taken as the state-of-the-art cation-water distance reported for solvated cations (see Table S3).<sup>5-6</sup>



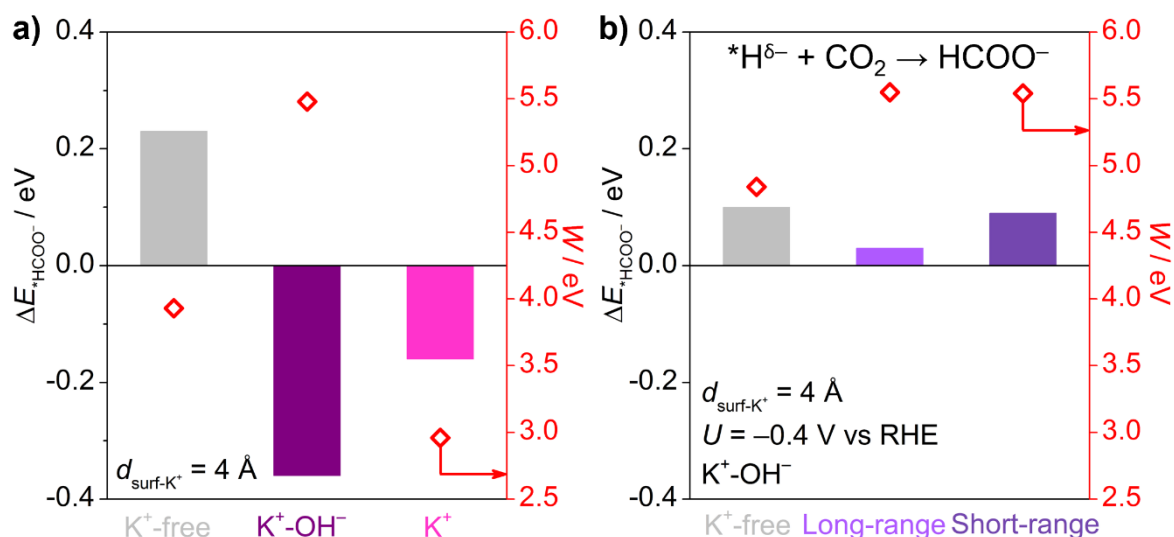


**Figure S13. a.** DFT energy on  $\text{Pd}_{\text{ML}}\text{Pt}(111)$  ( $3 \times 3$ ) relative to cation-induced outer-sphere  $\text{CO}_2$  activation to  $\text{HCOO}^-$  for the  $\text{K}^+$ -free (gray) and near- $\text{K}^+$  with and without balancing  $\text{OH}^-$  (purple and magenta) for different values of metal work functions (right y-axis). **b.** DFT energy relative to the  $\text{HCOO}^-$  formation step on  $\text{Pd}_{\text{ML}}\text{Pt}(111)$  ( $3 \times 3$ ) supercell for cation-free (gray), far- $\text{K}^+$  (light purple), and near- $\text{K}^+$  (dark purple) cases at  $U = -0.4 \text{ V vs RHE}$ . Values of metal work function for clean surfaces are given at the right y-axis. For details on the model, see Figure 5a-b and Computational Details.

**Table S1.** Calculated work function for the Pd<sub>ML</sub>Pt(111) (3×3) surface for clean surface and \*CO<sub>2</sub> for the K<sup>+</sup>-free, the near-K<sup>+</sup> ( $d_{K^+-surf} = 4 \text{ \AA}$ ), and far-K<sup>+</sup> ( $d_{K^+-surf} = 9 \text{ \AA}$ ) cases, with and without balancing OH<sup>-</sup>. Cation and H<sub>2</sub>O molecules (within bracket) were absent in the K<sup>+</sup>-free case.

| System   | W / eV               |                     |                                       |                    |                                       |
|--|----------------------|---------------------|---------------------------------------|--------------------|---------------------------------------|
|  | K <sup>+</sup> -free | Near K <sup>+</sup> | Near K <sup>+</sup> + OH <sup>-</sup> | Far K <sup>+</sup> | Near K <sup>+</sup> + OH <sup>-</sup> |
| Clean surface  | +4.84                | +2.35               | +5.54                                 | +1.74              | +5.55                                 |
| *CO <sub>2</sub> <sup>-</sup> (+ K <sup>+</sup> + 5H <sub>2</sub> O) | +5.05                | +5.09               | +5.59                                 | +5.14              | +5.41                                 |

**Table S2.** Calculated Bader charges of the Pd<sub>ML</sub>Pt(111) (3×3) surface for clean surface and \*CO<sub>2</sub> for the K<sup>+</sup>-free, the near-K<sup>+</sup> ( $d_{K^+-surf} = 4 \text{ \AA}$ ), and far-K<sup>+</sup> ( $d_{K^+-surf} = 9 \text{ \AA}$ ) cases, with and without balancing OH<sup>-</sup>. Cation and H<sub>2</sub>O molecules (within brackets) were absent in the K<sup>+</sup>-free case.

| System   | $q_{surf} /  e^- $   |                     |                                       |                    |                                       |
|--|----------------------|---------------------|---------------------------------------|--------------------|---------------------------------------|
|  | K <sup>+</sup> -free | Near-K <sup>+</sup> | Near K <sup>+</sup> + OH <sup>-</sup> | Far K <sup>+</sup> | Near K <sup>+</sup> + OH <sup>-</sup> |
| Clean surface  | +0.00                | -0.62               | -0.24                                 | -0.05              | -0.05                                 |
| *CO <sub>2</sub> <sup>-</sup> (+ K <sup>+</sup> + 5H <sub>2</sub> O) | +0.35                | -0.07               | +0.29                                 | +0.30              | +0.30                                 |

**Table S3.** Properties of alkali, bi-valent, and tri-valent cations, taken from Refs. <sup>5-8</sup>.

| Cation           | $q_{cat} /  e^- $ | ionic radius / $\text{\AA}$ | $d_{cat-O} / \text{\AA}$ | Acidity / $ e^- ^2 \text{\AA}^{-1}$ | $q_{cat}/r_{cat-O}^2 /  e^-  \text{\AA}^{-2}$ |
|------------------|-------------------|-----------------------------|--------------------------|-------------------------------------|---|
| Li <sup>+</sup>  | 1                 | 0.92                        | 2.08                     | 1.09                                | 0.23  |
| Na <sup>+</sup>  | 1                 | 1.39                        | 2.36                     | 0.72                                | 0.18  |
| K <sup>+</sup>   | 1                 | 1.64                        | 2.80                     | 0.61                                | 0.13  |
| Cs <sup>+</sup>  | 1                 | 1.88                        | 3.14                     | 0.53                                | 0.10  |
| Mg <sup>2+</sup> | 2                 | 0.89                        | 2.09                     | 4.49                                | 0.46  |
| Ba <sup>2+</sup> | 2                 | 1.61                        | 2.81                     | 2.48                                | 0.25  |
| Al <sup>3+</sup> | 3                 | 0.54                        | 1.89                     | 16.67                               | 0.84  |
| Nd <sup>3+</sup> | 3                 | 1.27                        | 2.47                     | 7.09                                | 0.49  |

## References

1. McCrum, I. T.; Koper, M. T. M., The role of adsorbed hydroxide in hydrogen evolution reaction kinetics on modified platinum. *Nature Energy* **2020**, *5* (11), 891-899.
2. Monteiro, M. C.; Dattila, F.; Hagedoorn, B.; García-Muelas, R.; López, N.; Koper, M., Absence of CO<sub>2</sub> electroreduction on copper, gold and silver electrodes without metal cations in solution. *Nat. Catal.* **2021**, *4* (8), 654-662.
3. Chan, K.; Nørskov, J. K., Potential Dependence of Electrochemical Barriers from ab Initio Calculations. *J. Phys. Chem. Lett.* **2016**, *7* (9), 1686-1690.
4. Chan, K.; Nørskov, J. K., Electrochemical Barriers Made Simple. *J. Phys. Chem. Lett.* **2015**, *6* (14), 2663-2668.
5. Monteiro, M. C. O.; Dattila, F.; Lopez, N.; Koper, M. T. M., The Role of Cation Acidity on the Competition between Hydrogen Evolution and CO<sub>2</sub> Reduction on Gold Electrodes. *J. Am. Chem. Soc.* **2022**, *144* (4), 1589-1602.
6. Marcus, Y., Ionic radii in aqueous solutions. *Chem. Rev.* **1988**, *88* (8), 1475-1498.
7. Haynes, W. M., *CRC handbook of chemistry and physics*. CRC press: 2016.
8. Waegele, M. M.; Gunathunge, C. M.; Li, J.; Li, X., How cations affect the electric double layer and the rates and selectivity of electrocatalytic processes. *J. Chem. Phys.* **2019**, *151* (16), 160902.